Rap1 binding to the talin 1 F0 domain makes a minimal contribution to murine platelet GPIIb-IIIa activation

Frederic Lagarrigue,[1] Alexandre R. Gingras,[1] David S. Paul,[2] Andrew J. Valadez,[1] Monica N. Cuevas,[1] Hao Sun,[1] Miguel A. Lopez-Ramirez,[1] Benjamin T. Goult,[3] Sanford J. Shattil,[1] Wolfgang Bergmeier,[2,4] and Mark H. Ginsberg[1]

[1]Department of Medicine, University of California, San Diego, La Jolla, CA; [2]McAllister Heart Institute, University of North Carolina at Chapel Hill, Chapel Hill, NC; [3]School of Biosciences, University of Kent, Kent, United Kingdom; and [4]Department of Biochemistry and Biophysics, University of North Carolina at Chapel Hill, Chapel Hill, NC

Key Points

- Platelets expressing a talin 1 mutant (R35E) that significantly reduces Rap1 affinity exhibit little change in GPIIb-IIIa activation.

- $Tln1^{R35E/R35E}$ mice are viable, apparently healthy, and fertile, with similar bleeding times as wild-type littermates.

Activation of platelet glycoprotein IIb-IIIa (GPIIb-IIIa; integrin αIIbβ3) leads to high-affinity fibrinogen binding and platelet aggregation during hemostasis. Whereas GTP-bound Rap1 GTPase promotes talin 1 binding to the β3 cytoplasmic domain to activate platelet GPIIb-IIIa, the Rap1 effector that regulates talin association with β3 in platelets is unknown. Rap1 binding to the talin 1 F0 subdomain was proposed to forge the talin 1–Rap1 link in platelets. Here, we report a talin 1 point mutant (R35E) that significantly reduces Rap1 affinity without a significant effect on its structure or expression. Talin 1 head domain (THD) (R35E) was of similar potency to wild-type THD in activating αIIbβ3 in Chinese hamster ovary cells. Coexpression with activated Rap1b increased activation, and coexpression with Rap1GAP1 reduced activation caused by transfection of wild-type THD or THD(R35E). Furthermore, platelets from $Tln1^{R35E/R35E}$ mice showed similar GPIIb-IIIa activation to those from wild-type littermates in response to multiple agonists. $Tln1^{R35E/R35E}$ platelets exhibited slightly reduced platelet aggregation in response to low doses of agonists; however, there was not a significant hemostatic defect, as judged by tail bleeding times. Thus, the Rap1–talin 1 F0 interaction has little effect on platelet GPIIb-IIIa activation and hemostasis and cannot account for the dramatic effects of loss of Rap1 activity on these platelet functions.

Introduction

Platelet aggregation, which is essential for normal hemostasis,[1] is initiated by agonists, such as thrombin or collagen, resulting in activation of glycoprotein IIb-IIIa (GPIIb-IIIa; integrin αIIbβ3) to bind fibrinogen with high affinity.[2] GPIIb-IIIa activation depends on binding of talin 1 to the integrin β3 cytoplasmic tail.[3] Rap1 GTPases are important intermediaries in integrin activation. In particular, mice deficient in Rap1b, the most abundant isoform of Rap1 in platelets, or its main activator CalDAG-GEF1, exhibit impaired GPIIb-IIIa activation.[4,5] Moreover, platelet-specific deletion of Rap1a and Rap1b leads to a profound defect in GPIIb-IIIa activation and hemostasis.[6] RIAM is a Rap1 effector that recruits talin 1 to integrin αIIbβ3 in a model nonhematopoietic system.[7-9] However, genetic ablation of RIAM in mice does not affect hemostasis or GPIIb-IIIa activation, indicating that it is not the relevant Rap1 effector in platelets.[10-12]

The N-terminal talin 1 head domain (THD) is an atypical FERM domain with an F0 domain, in addition to the 3 characteristic subdomains (F1, F2, F3). The structure of the F0 domain resembles that of the Ras-association domain in RalGDS, and Rap1 binds weakly to talin 1 F0 (dissociation constant [K_d] ~140 μM) in a guanosine triphosphate–dependent manner.[13] In *Dictyostelium*, Rap1 binds to the Ras-association domain of talinB to mediate cellular adhesion during morphogenesis.[14] The low-affinity binding of talin 1 F0 to Rap1 was confirmed by a recent study that suggested that this was the Rap1–talin 1 interaction that mediates platelet GPIIb-IIIa activation.[15] Here, we analyzed the effect of F0 mutations that disrupt Rap1

binding on the ability of THD to activate integrin αIIbβ3 in a CHO cell system. These mutations did not affect αIIbβ3 activation, nor did they alter the effect of manipulation of Rap1 activity on αIIbβ3 activation. We generated $Tln1^{R35E/R35E}$ mice harboring a mutation that significantly reduces the affinity of talin 1 F0 for Rap1. Initial platelet GPIIb-IIIa activation and hemostasis were similar in $Tln1^{R35E/R35E}$ mice and wild-type littermates; however, platelet aggregation in response to low doses of agonists was reduced. Thus, Rap1 binding to talin 1 F0 cannot account for the dramatic effects of the loss of Rap1 activity on GPIIb-IIIa activation and hemostasis.

Methods

Reagents

Prostacyclin (PGI$_2$), adenosine 5$'$-diphosphate, thrombin, and calcium ionophore A23187 were from Sigma-Aldrich. Protease-activated receptor 4–activating peptide (PAR4-AP, AYPGKF-NH$_2$) was from GenScript. Cross-linked collagen-related peptide (CRP-XL) was from the University of Cambridge (Department of Biochemistry). Fibrillar collagen type I was from Chrono-log. U46619 was from Cayman Chemical.

Protein expression and purification

The murine talin 1 residues 1-85 (F0) were cloned into the expression vector pETM-11 (His-tagged, EMBL) and expressed in *Escherichia coli* BL21 Star (DE3) cultured in minimal medium for ^{15}N-labeled samples for nuclear magnetic resonance (NMR). Briefly, recombinant His-tagged F0 was purified by nickel-affinity chromatography, the His-tag was removed by cleavage with Tobacco Etch Virus protease overnight, and the protein was further purified by size-exclusion chromatography using a Superdex 75 (26/600) column (GE Healthcare). The column was pre-equilibrated and run with (NMR buffer) 20 mM sodium phosphate, 50 mM NaCl, 3 mM MgCl$_2$, 2 mM dithiothreitol, pH 6.5. Human Rap1 isoform Rap1b (residues 1-167) cloned into pTAC vector in the *E coli* strain CK600K was the generous gift of Professor Alfred Wittinghofer (Max Planck Institute of Molecular Physiology, Dortmund, Germany). Untagged Rap1b was purified by ion exchange, followed by Superdex 75 (26/600) gel filtration, as previously described.[16] The column was pre-equilibrated and run with NMR buffer.

NMR titration

Titration curves for the interaction of talin 1 F0 with GMP.PNP-bound Rap1b were determined using 100 μM ^{15}N-labeled F0 in NMR buffer containing 5% (v/v) ^{2}H$_2$O. All 2-dimensional (2D) [^{1}H,^{15}N]-sfHMQC spectra were recorded at 298 K. Chemical shift changes [$\Delta\delta_{obs\ (HN,N)}$] were calculated using CcpNmr Analysis "follow shift changes" function and analyzed with the 1-site binding model to determine the K_d value in Prism 5.0 (GraphPad Software).[17]

Integrin activation in Chinese hamster ovary cells

Cells were cultured in Dulbecco's modified Eagle medium (Corning) supplemented with 10% fetal bovine serum (Sigma-Aldrich), 100 U/mL penicillin, and 100 μg/mL streptomycin (Gibco). The sequence encoding murine THD (amino acids 1-433) was cloned into pEGFP-N1 (Clontech). Point mutations were incorporated by PCR using gBlocks gene fragment (IDT) as templates. The sequences encoding human Rap1b(Q63E) and Rap1GAP1 were cloned into pDsRed-Monomer-C1 (Clontech). Transient transfection was performed using TransIT-LT1 Transfection Reagent (Mirus), according to the manufacturer's protocol. PAC-1 binding assay was conducted as

previously described.[18] Briefly, cells were harvested using trypsin 1 day after transfection and washed once in Hanks balanced salt solution buffer (containing calcium and magnesium; Gibco) supplemented with 1% (w/v) bovine serum albumin (BSA; Sigma-Aldrich). PAC-1 immunoglobulin M (ascites, 1:200) was incubated with cells for 30 minutes at room temperature prior to staining with the appropriate Alexa Fluor 647 secondary antibody (Life Technologies) for 30 minutes on ice. Cells were analyzed by flow cytometry using a FACSAria (BD Biosciences) and gated on double EGFP/DsRed$^+$ events. Integrin activation was defined as αIIbβ3-specific ligand binding corrected for αIIbβ3 expression and was calculated as $100 \times (MFI_i - MFI_0)/\Delta MFI_{D57}$ (MFI_i = mean fluorescence intensity [MFI] of bound PAC-1, MFI_0 = mean fluorescence intensity of bound PAC-1 in the presence of 10 μM eptifibatide, and ΔMFI_{D57} = specific fluorescence intensity of anti-αIIbβ3 D57 antibody). PAC1[19] and D57[20] antibodies have been previously described.

Mice

$Tln1^{R35E/R35E}$ mice were generated by the CRISPR/Cas9 approach at the University of California Irvine Transgenic Mouse Facility (UCI TMF). $Apbb1ip^{-/-10,12}$ and $Tln2^{-/-21}$ mice have been described. Eight- to 16-week-old sex-matched wild-type littermates were used as control animals for all experiments. $Tln1^{R35E/R35E}$ knock-in mice were generated using a CRISPR/Cas9 approach at the UCI TMF. The single guide RNA and the single-stranded oligonucleotides were from IDT. Cas9 mRNA/ single guide RNA/tracRNA (3 μM) was mixed with single-stranded oligonucleotides (5 ng/μL) and injected into the pronuclei of B6SJLF2 embryos. Surviving embryos were implanted into ICR pseudopregnant females, and pregnancies went to full term. Tissue biopsies for genomic DNA were taken from pups between 7 and 10 days. Mice were genotyped by polymerase chain reaction using forward primer 5$'$-gtattctaatgctctgatgctactggc-3$'$ and reverse primer 5$'$-aaagtcgttggc-taaaagagatggtag-3$'$, followed by Sanger sequencing. Three founder $Tln1^{R35E/R35E}$ mice were backcrossed to a C57BL/6 strain to obtain heterozygous $Tln1^{wt/R35E}$ mice. We used sex-matched $Tln1^{wt/wt}$ littermates as controls for $Tln1^{R35E/R35E}$ mutant animals in all experiments. Mice were housed in the animal facilities of the University of California, San Diego. Experimental procedures were approved by the Institutional Care and Use Committee.

Blood counts

Peripheral blood was collected from the retro-orbital plexus and transferred to tubes containing EDTA. Cell counts were performed using a Hemavet 950FS hematology system programmed with mouse-specific settings (Drew Scientific). All samples were tested in duplicate, and the mean for each animal was plotted.

Platelet preparation

Blood was drawn with heparin-coated capillaries (VWR) from the retro-orbital plexus into tubes containing low-molecular-weight LOVENOX (enoxaparin sodium; Sanofi-Aventis). Whole blood was diluted with modified Tyrode's buffer (137 mM NaCl, 0.3 mM Na$_2$HPO$_4$, 2 mM KCl, 12 mM NaHCO$_3$, 5 mM *N*-2-hydroxyethylpiperazine-N$'$-2-ethanesulfonic acid, 5 mM glucose, pH 7.3) containing 0.35% BSA. Platelet-rich plasma (PRP) was obtained by 2 successive centrifugation steps at 130g for 4 minutes and then at 100g for 5 minutes at room temperature. PRP was centrifuged at 700g for 5 minutes at room temperature in the presence of 5 μM PGI$_2$ to pellet platelets. Platelets were resuspended in modified Tyrode's buffer, and platelet concentration was adjusted to 5 $\times$ 10^8/mL.
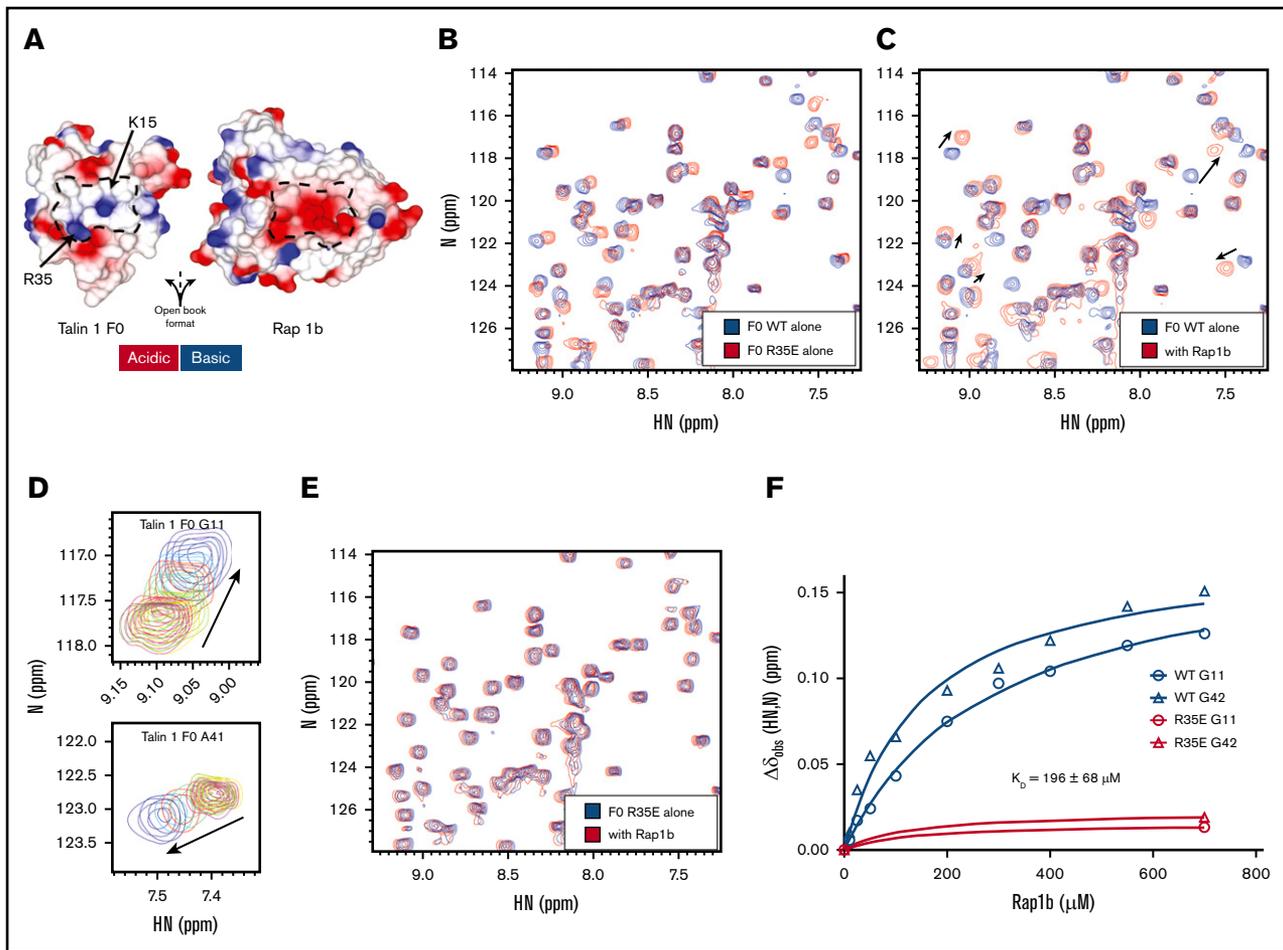
Figure 1. Biochemical characterization of the talin 1 R35E mutation to block binding to Rap1b. (A) Surface electrostatic potential of talin 1 F0 (left panel) and Rap1b (right panel) binding interface as open book view. The charge complementarity between the 2 proteins' binding interface is represented by the dashed line. (B-E) 2D NMR ^{1}H,^{15}N-sfHMQC spectra (298K, 600 MHz) of 100 μM ^{15}N-labeled talin 1 F0. (B) Free talin 1 F0 wild-type (blue) and R35E (red). Almost all peaks are in the same position, suggesting that THD(R35E) is well folded and has a fold similar to wild-type protein. (C) Talin 1 F0 wild-type (blue); with sevenfold excess Rap1b (red), specific chemical shift changes are observed and indicated by arrows. (D) Close-up view of the 10-step Rap1b titration for residues G11 and A41. (E) Talin 1 F0(R35E) (blue); in the presence of sevenfold excess Rap1b (red), minimal chemical shift changes are observed, showing that THD(R35E) drastically reduced interaction. (F) Titration curves for the interaction of talin 1 F0 wild-type (blue) or R35E (red) (100 μM) with increasing amounts of Rap1b (0-700 μM). Wild-type dissociation constants were measured for multiple residues, and binding curves are shown for G11 and G42 talin 1 F0 wild-type and mutant proteins. The F0(R35E) affinity for Rap1b was dramatically reduced (at 700 μM Rap1b, no binding was detected).

Flow cytometry

Washed platelets were diluted to 4×10^7/mL in Tyrode's solution containing 1 mM $CaCl_2$ with agonists in the presence of fibrinogen conjugated to Alexa Fluor 488 (150 μg/mL; Life Technologies). After 10 minutes of incubation, each sample was further diluted 1:40 in phosphate buffered saline (PBS) and analyzed immediately with a BD Accuri C6 Plus flow cytometer (BD Biosciences). For whole-blood assays, blood was diluted 1:12.5 in modified Tyrode's solution containing 1 mM $CaCl_2$ with agonists in the presence of Jon/A-phycoerythrin (PE) (2 μg/mL) and GPIX labeled with Alexa Fluor 647 (2 μg/mL), incubated for 10 minutes at room temperature, and diluted 1:400 in PBS prior to fluorescence-activated cell sorting. For real-time GPIIb-IIIa activation assay, washed platelets were diluted in modified Tyrode's solution containing 1 mM $CaCl_2$. After establishing a baseline with unlabeled platelets for 30 seconds, Jon/A-PE and PAR4-AP agonist were added simultaneously in an equal volume of modified Tyrode's

solution. Jon/A-PE binding was recorded continuously for 10 minutes. Monoclonal antibodies directed against GPIX (Xia.B4) or activated murine GPIIb-IIIa (Jon/A-PE) were from emfret Analytics. For surface receptor analysis, 2×10^6 platelets in diluted whole blood (modified Tyrode's buffer) were stained for 10 minutes with 2 μg/mL fluorophore-conjugated antibodies and immediately analyzed by flow cytometry. PE-conjugated antibodies against CD41 (MWReg30; control isotype RTK2071) and CD61 (2C9.G2; control isotype HTK888) were from BioLegend. Fluorescein isothiocyanate–conjugated antibody against P-selectin (CD62P, RB40.34; control isotype A110-1) was from BD Biosciences.

Aggregometry

PRP was diluted to a concentration of 2×10^8 platelets/mL in modified Tyrode's buffer containing 0.35% BSA and 1 mM $CaCl_2$. The experiment was performed at 37°C under stirring conditions (1200 rpm). Platelets were stimulated with various concentrations
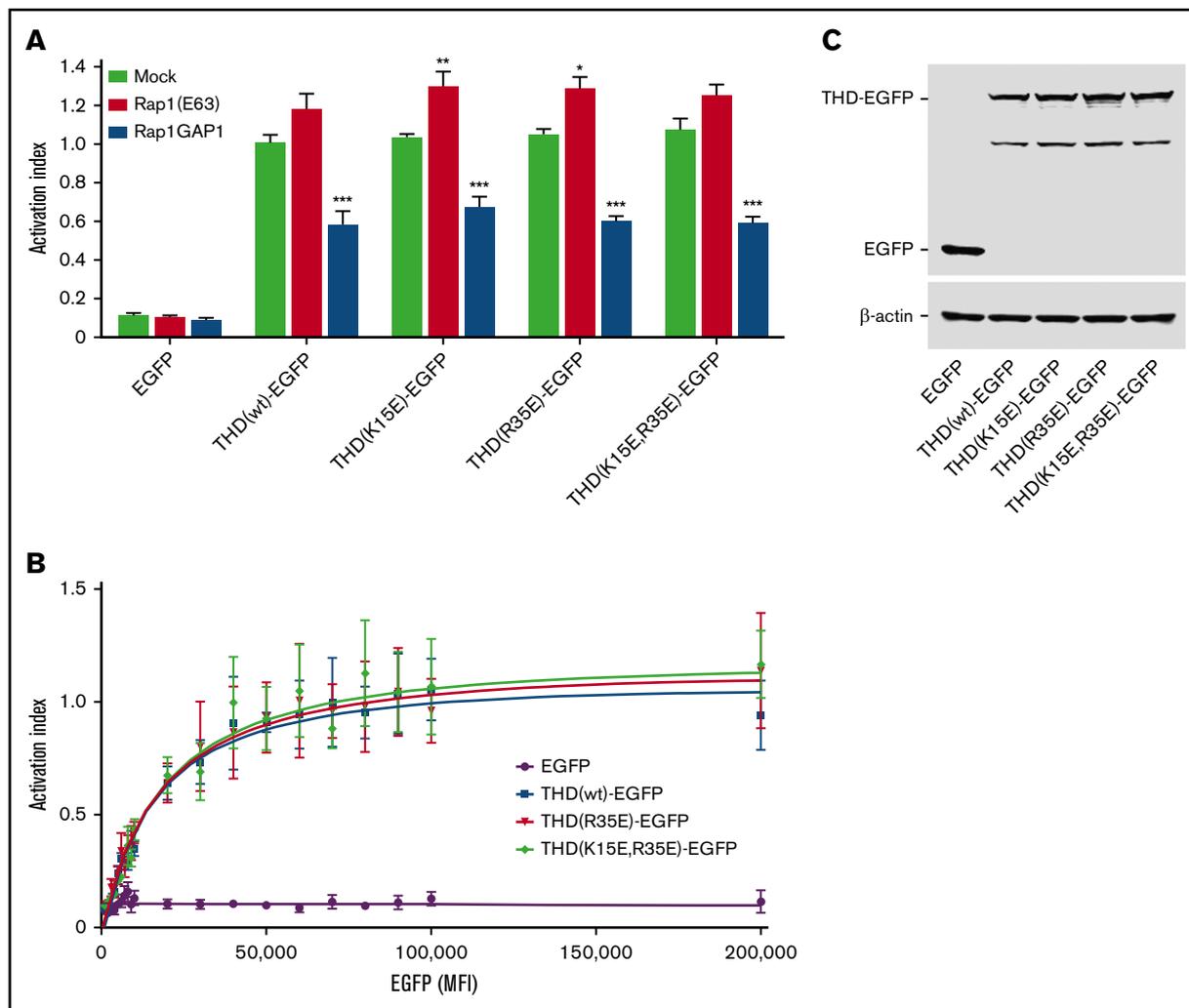
Figure 2. Talin 1 R35E mutation does not impede αIIbβ3 integrin activation in CHO cells. (A) CHO-A5 cells stably expressing αIIbβ3 integrin were transfected with complementary DNA encoding EGFP-tagged THD in combination with Rap1b(Q63E) or Rap1GAP1. Integrin activation was assayed by binding of PAC1 to EGFP^{+} cells. Bar graph shows mean ± standard error of the mean (SEM) of 4 independent experiments. No significant differences between wild-type and mutants were detected. (B) Activation indices were normalized to the maximum value of THD(wild-type)–EGFP and plotted as a function of EGFP-MFI. Graphs represent mean ± SEM of 4 independent experiments. Curve fitting was performed using the total 1 site-binding model in Prism 5.0 (GraphPad Software). No significant difference between wild-type and mutants was detected. (C) Expression of EGFP-THD mutants was assayed by western blotting. *$P < .05$, **$P < .01$, ***$P < .001$, 2-way analysis of variance with Bonferroni posttest.

of PAR4-AP. Light transmission was recorded on a Chrono-log 4-channel optical aggregation system (Chrono-log).

Tail bleeding time assay

Mice were anesthetized, and a 5-mm segment of the tail tip was cut off with a scalpel. The tail was immediately immersed in isotonic saline prewarmed to 37°C. Bleeding times were the time required for bleeding to cease for ≥60 seconds.

Platelet static adhesion to fibrinogen

Glass coverslips were coated with 100 μg/mL fibrinogen (Sigma-Aldrich) in PBS for 1 to 2 hours at 37°C, washed twice with PBS, and blocked with 5% BSA/PBS for 2 hours at 37°C. Washed platelets were diluted 1:10 in Tyrode's solution containing 1 mM $CaCl_2$ in the presence of 0.01 U/mL thrombin and left to adhere to fibrinogen-coated glass coverslips for various times. Wells were washed 3 times with Tyrode's

solution. Adherent platelets were fixed with formaldehyde, stained with Alexa Fluor 488 phalloidin (Life Technologies), and imaged using an LSM 880 with Airyscan confocal microscope (63×/1.4 oil objective; Carl Zeiss). The number of attached platelets and the spreading area were measured using the ImageJ image analysis software.

Western blotting

Washed platelets were pelleted by centrifugation at 700g for 5 minutes at room temperature and then lysed in Laemmli sample buffer. Lysates were subjected to 4% to 20%–gradient sodium dodecyl sulfate–polyacrylamide gel electrophoresis. For analysis of talin levels, platelet lysates were subjected to 6% sodium dodecyl sulfate–polyacrylamide gel electrophoresis for better protein separation. Antibodies directed against talin 1 (93E12) and talin 2 (68E7) were from Novus Biologicals. Anti-Rap1A/B was from Cell Signaling Technology (#4938). Antibodies against vinculin (hVIN-1)
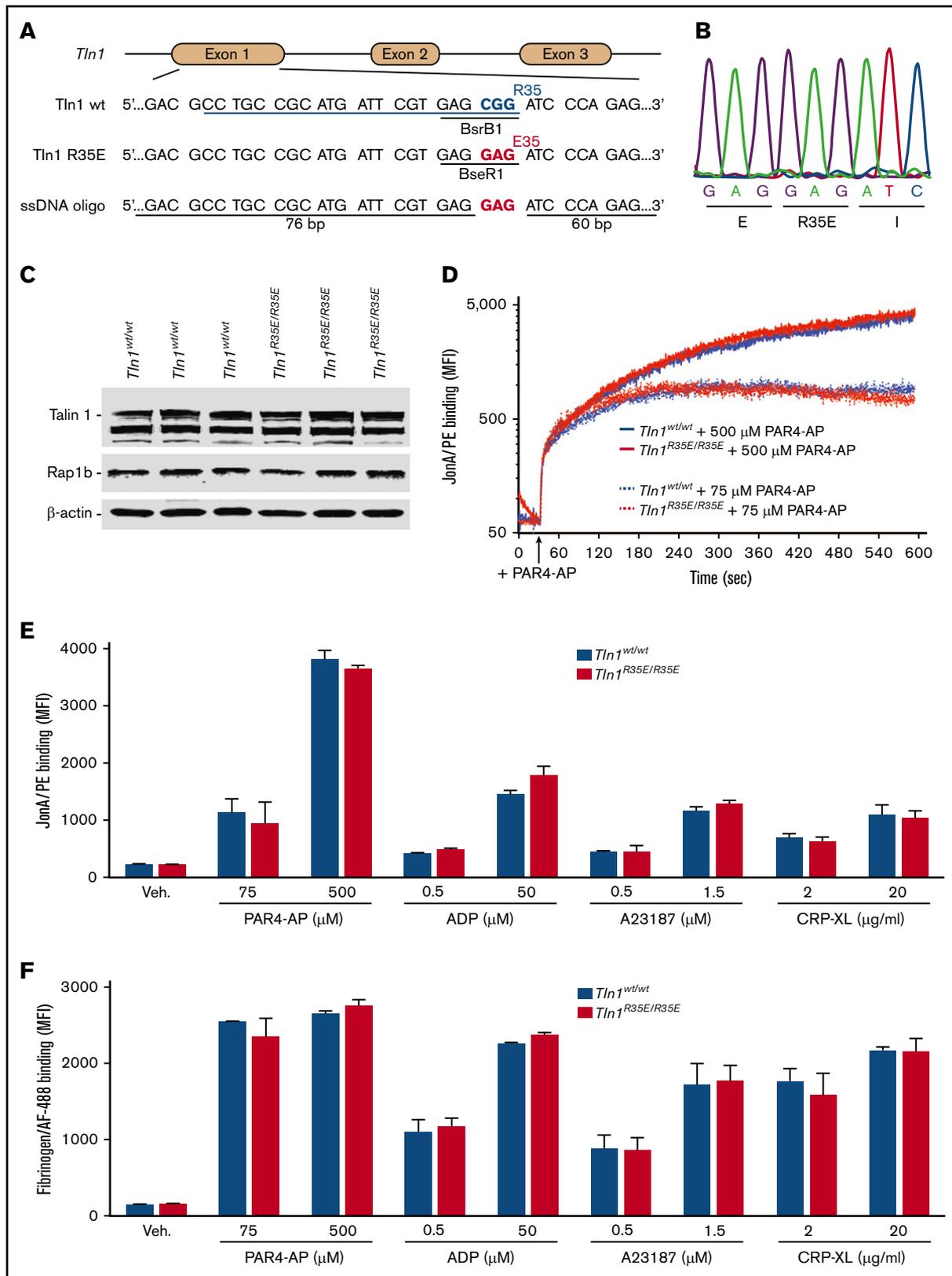
Figure 3. Platelets expressing talin 1(R35E) exhibit normal GPIIb-IIIa integrin activation. (A) Generation of mice expressing talin 1(R35E) mutant. (B) Sequencing chromatogram of the mutated region of *Tln1(R35E)* gene. (C) Expression of talin 1(R35E) mutant in platelets was assayed by western blotting. Results are representative of 3 independent experiments, n = 3 mice each time. (D-F) Normal GPIIb-IIIa integrin activation in *Tln1$^{R35E/R35E}$* platelets. (D) Real-time GPIIb-IIIa activation assay. Jon/A-PE binding to washed platelets was recorded continuously for 10 minutes by flow cytometry. Jon/A antibody was added at the time of stimulation with 75 or 500 μM PAR4-AP (indicated
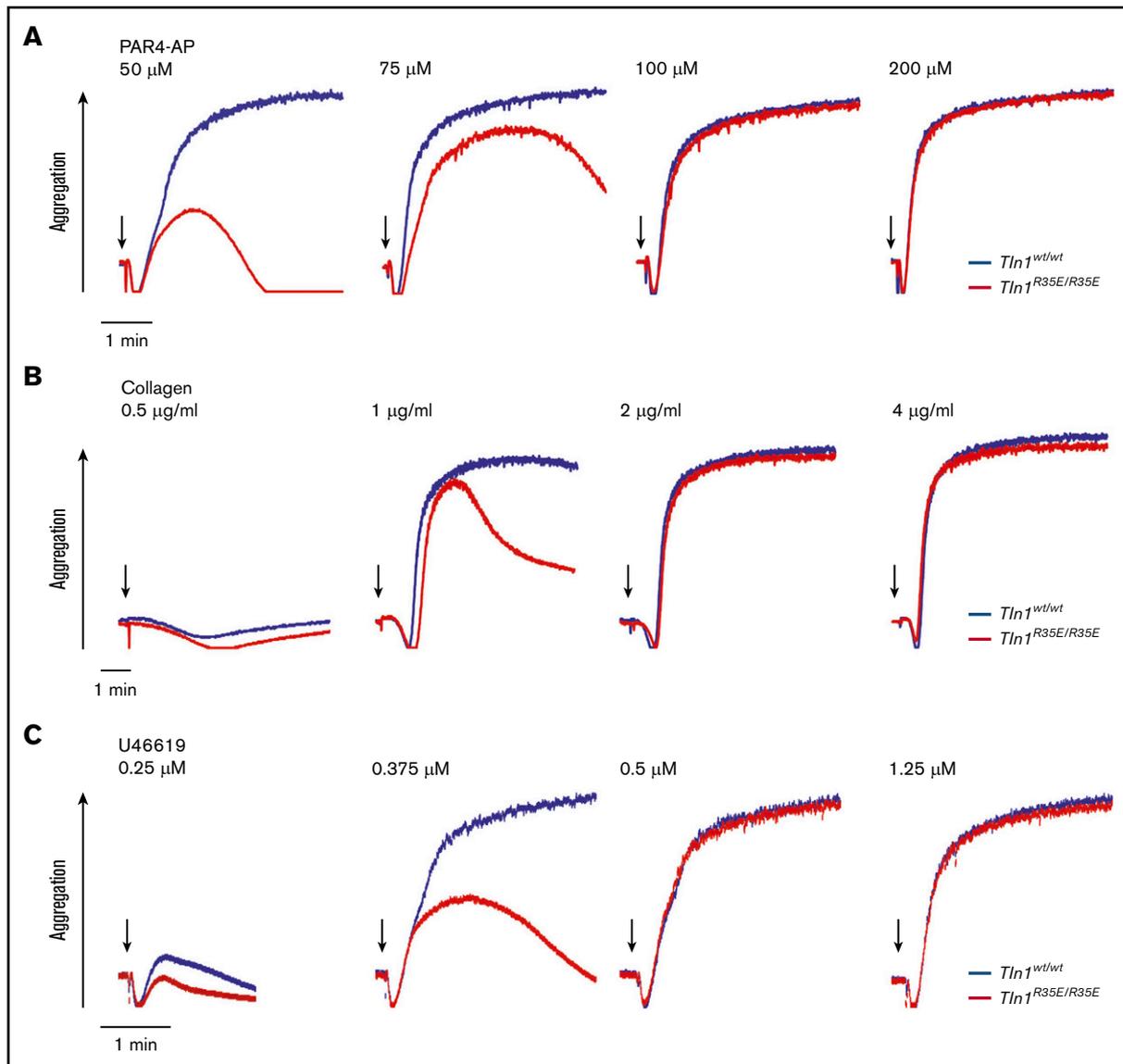
Figure 4. Unstable aggregation of *Tln1^R35E/R35E* platelets in response to stimulation with a low dose of agonists. Aggregation of *Tln1^wt/wt* and *Tln1^R35E/R35E* platelets stimulated with various doses of PAR4-AP (A), fibrillar collagen type I (B), and the thromboxane A2 analog U46619 (C). Arrows indicate addition of the agonist. Results are representative of 3 independent experiments, n = 3 mice each time.

and β-actin (AC-15) were from Sigma-Aldrich. The appropriate IRDye/Alexa Fluor–coupled secondary antibodies were from LI-COR. Nitrocellulose membranes were scanned using an Odyssey CLx Infrared Imaging System, and blots were processed using Image Studio Lite software (both from LI-COR).

Statistics

Statistical significance was assayed by a 2-tailed Student *t* test for single comparisons or analysis of variance for multiple comparisons with a Bonferroni post hoc test. $P < .05$ was considered significant.

Results

Reduced affinity of talin 1(R35E) F0 domain binding to Rap1

Our molecular modeling and a published NMR structure[15] suggested that talin 1 Lys15 and Arg35 formed crucial salt bridges with an acidic patch on Rap1b (Figure 1A). We prepared K15E and R35E mutants of F0 and noted that the R35E mutant was more stable when expressed in bacteria. Comparison of the NMR 2D-sfHMQC of the F0 wild-type and R35E mutant (Figure 1B) showed

---

Figure 3. (continued) by the arrow). Flow cytometry assay to measure binding of GPIX-labeled platelets in whole blood to Jon/A antibody (E) or washed platelets to fibrinogen (F) in response to agonist stimulation. Alexa Fluor 488–coupled fibrinogen and Jon/A-PE were added simultaneously with agonists for 10 minutes. Bar graphs represent MFI ± standard error of the mean (n = 4 mice, representative of ≥4 independent experiments).
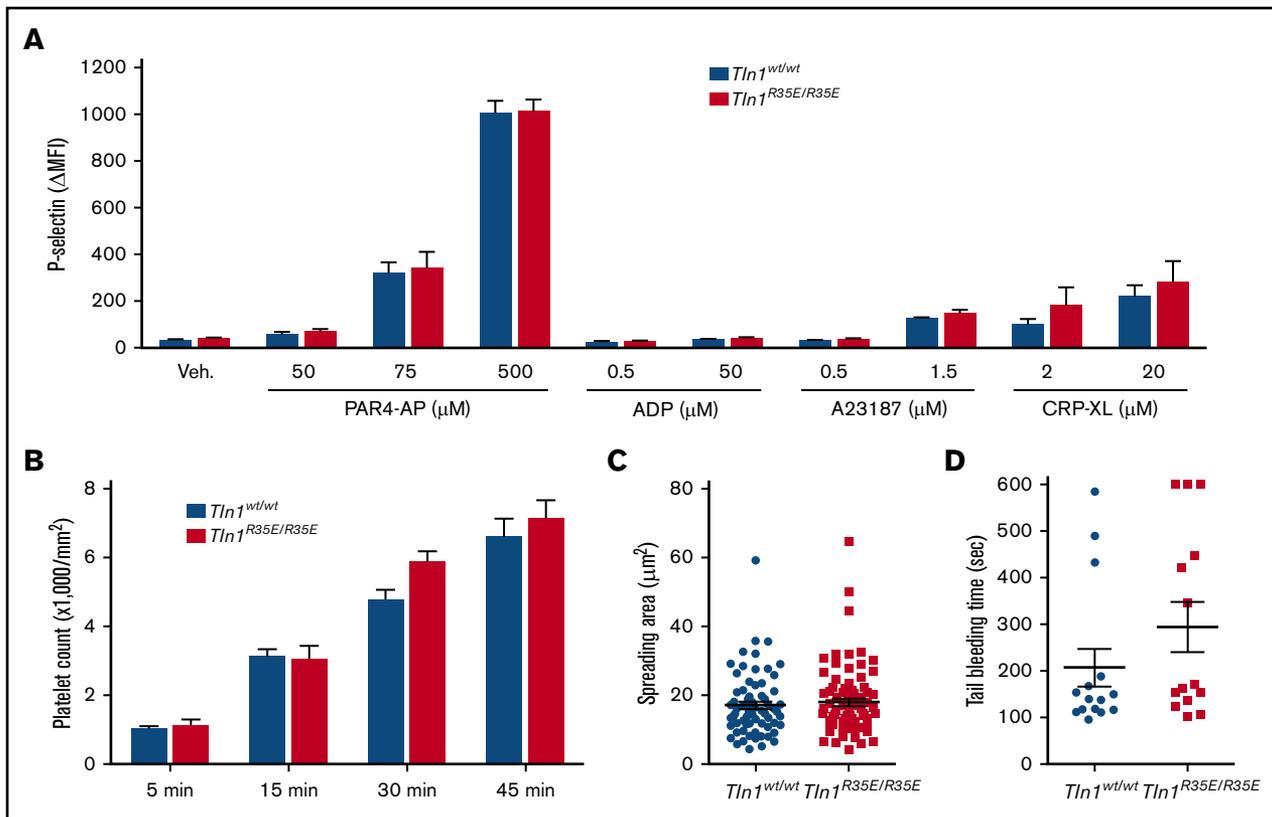
Figure 5. Analysis of platelet adhesion and secretion, as well as hemostasis, in *Tln1^R35E/R35E* mice. (A) P-selectin (CD62P) surface expression onto platelets in whole blood. Bar graph represents ΔMFI ± SEM (n = 4 mice, representative of 2 independent experiments). (B-C) Adhesion of *Tln1^R35E/R35E* platelets onto fibrinogen-coated surfaces. Washed platelets were stimulated with thrombin (0.01 U/mL). Platelets were pooled from 3 mice, 2 independent experiments. (B) Bar graphs are mean ± SEM of adhered platelet counts at the indicated time points after stimulation. (C) Quantification of platelet area at 45 minutes. Data are mean ± SEM. (D) Tail bleeding analysis. The experiment was terminated at the end of 10 minutes to avoid excessive loss of blood. No significant differences were observed between *Tln1^wt/wt* mice (n = 15) and *Tln1^R35E/R35E* mice (n = 14).

only very subtle chemical shift changes; thus, the mutant protein adopts a similar fold to wild-type F0. Addition of GMP.PNP Rap1b to F0 produced specific chemical shift changes detectable at 25 µM GMP.PNP Rap1b (Figure 1C-D,F), whereas addition of GMP.PNP Rap1b to F0(R35E) produced almost none at 700 µM GMP.PNP Rap1b (Figure 1E-F). Furthermore, we mapped specific chemical shifts to amino acids located in the predicted binding interface, including Lys15 and Arg35. NMR titrations, based on the fitting of chemical shift perturbations of amino acids located at the binding interface, showed a weak affinity of talin 1 F0 for Rap1b. Based on this standard method of NMR titration,[15] we calculated $K_d = 196 \pm 68$ µM (Figure 1F, blue lines). The minimal chemical shift perturbations detected in talin 1 F0(R35E) at 700 µM Rap1b (sevenfold excess) precluded calculation of K_d, but it did indicate a dramatic reduction in Rap1b affinity (Figure 1F). Thus, talin 1 F0(R35E) is well folded and binds to activated Rap1b with greatly reduced affinity.

Talin 1 F0–Rap1b interaction is dispensable for THD-mediated αIIbβ3 activation in CHO cells

To assess the contribution of the talin 1 F0 interaction with Rap1 on integrin activation, we introduced the mutations K15E and/or R35E into the THD and tested effects on integrin activation in Chinese hamster ovary (CHO) A5 cells stably expressing human αIIbβ3.

Expression of wild-type THD induced activation (Figure 2A). Expression of the constitutively activated Rap1b(E63) mutant, which is unable to form the Rap1-Rap1GAP1 complex,[22] increased wild-type THD-mediated αIIbβ3 activation. Inhibition of endogenous Rap1 activity by coexpression of Rap1GAP1 led to a decrease in THD-mediated activation (Figure 2A). THD(K15E), THD(R35E), or THD(K15E,R35E) mutants were similar to wild-type THD in activating αIIbβ3 and in the effect of manipulating Rap1 activity (Figure 2A). Furthermore, we carefully monitored expression of THD-EGFP and its mutants in each cell by flow cytometry and observed no differences in their capacity to activate αIIbβ3, regardless of their abundance (Figure 2B). Immunoblotting confirmed a similar level of expression for all THD mutants (Figure 2C).

Generation of *Tln1^R35E* knock-in mice

A striking feature of platelets is the abundance of Rap1b and talin 1, with ∼220 000 molecules per platelet.[23] Hence, the low-affinity talin 1–Rap1b interaction could regulate GPIIb-IIIa in platelets. To test this hypothesis, we used CRISPR/Cas9 to generate *Tln1^R35E/R35E* mice (Figure 3A-B). Homozygous *Tln1^R35E/R35E* mice were viable and fertile and exhibited no gross developmental abnormalities, with normal platelet and blood cell counts (supplemental Figure 1). Platelet content of talin 1, Rap1b (Figure 3C), and surface integrin GPIIb-IIIa (supplemental Figure 2) was similar to wild-type

Figure 6. GPIIb-IIIa activation in *Tln1^R35E/R35E* , *Apbb1ip^KO/KO* (RIAM-null) platelets. (A) Western blot analysis of talin 1 and RIAM expression in platelets. Vinculin was used as a loading control. (B-C) Normal GPIIb-IIIa integrin activation in *Tln1^R35E/R35E*, *Apbb1ip^−/−* platelets. Flow cytometry assay to measure binding of washed platelets to fibrinogen (B) or GPIX-labeled platelets in whole blood to Jon/A antibody (C). Bar graphs represent MFI ± SEM (n = 4 mice, representative of 2 independent experiments).
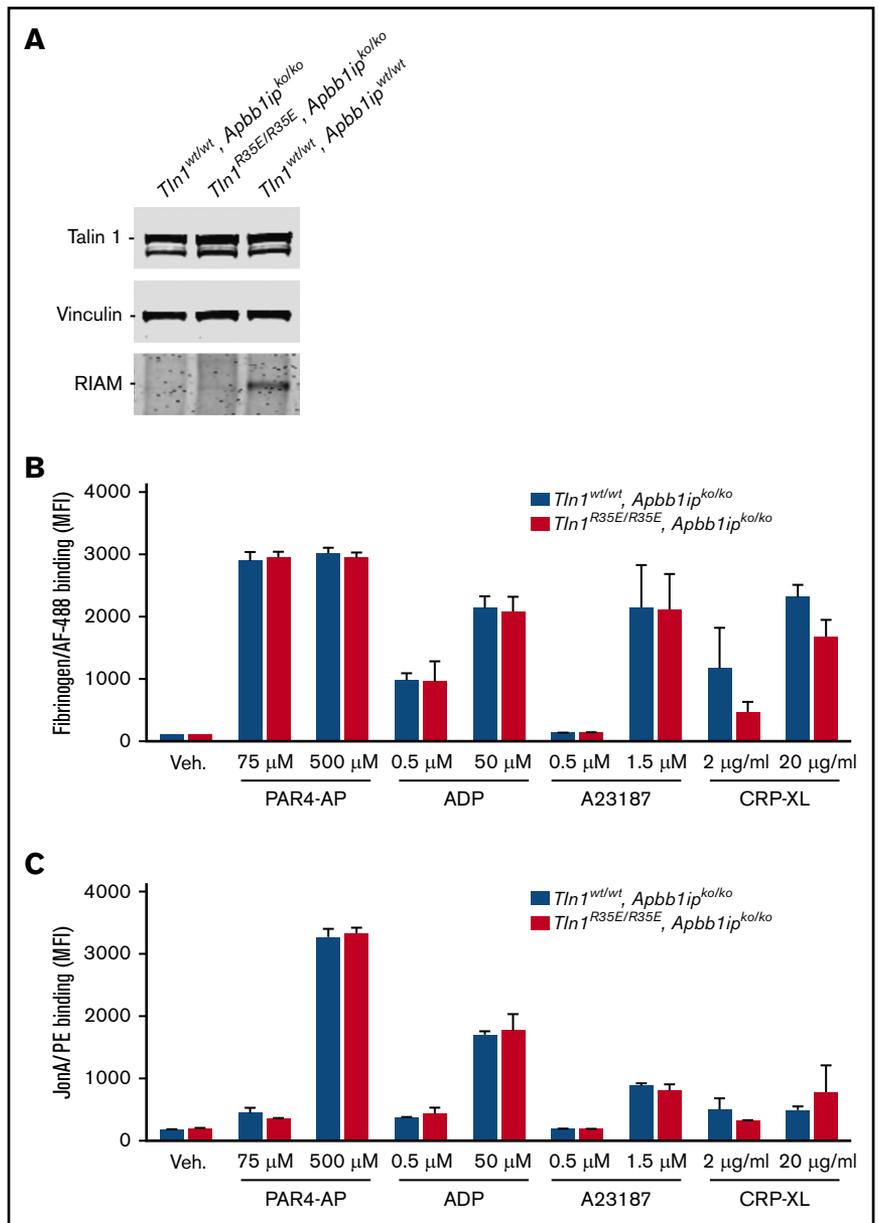
mice. Thus, *Tln1^R35E/R35E* mice are suitable for examining the effects of blocking Rap1 binding to the talin 1 F0 domain on platelet integrin function in vivo and ex vivo.

Normal agonist-induced GPIIb-IIIa activation of *Tln1^R35E/R35E* platelets

We evaluated activation of GPIIb-IIIa in response to stimulation with PAR4 agonist-peptide (PAR4-AP) by measuring real-time binding of Jon/A[24] to washed platelets and observed that Jon/A bound to PAR4-AP–activated *Tln1^R35E/R35E* platelet GPIIb-IIIa with similar kinetics and to a similar extent as wild-type platelets (Figure 3D). To rule out a platelet-washing artifact, we assessed GPIIb-IIIa activation in whole blood using Jon/A and found that multiple agonists stimulated Jon/A binding to *Tln1^R35E/R35E* platelets indistinguishably from wild-type platelets (Figure 3E). As a second measure of GPIIb-IIIa activation, we assessed fibrinogen binding to washed platelets and found that binding to *Tln1^R35E/R35E* platelets stimulated with PAR-AP, adenosine 5′-diphosphate, ionophore A23187, or collagen-related peptide was similar to fibrinogen binding to platelets from wild-type mice (Figure 3F). Thus, these data indicate that Rap1 binding to talin 1 F0 domain is dispensable for GPIIb-IIIa activation in platelets.

Mild defect in aggregation of *Tln1^R35E/R35E* platelets

To examine the ability of *Tln1^R35E/R35E* platelets to form aggregates, we stimulated diluted PRP in a standard optical aggregometer with various doses of PAR4-AP, collagen, or the thromboxane A2 analog U46619. There was a consistent reduction in the ability of low doses of agonists to induce *Tln1^R35E/R35E* platelet aggregation (Figure 4). Surface expression of P-selectin in *Tln1^R35E/R35E* platelets was similar to platelets from wild-type mice (Figure 5A), indicating no defect in α-granule secretion. In addition, as an independent measure
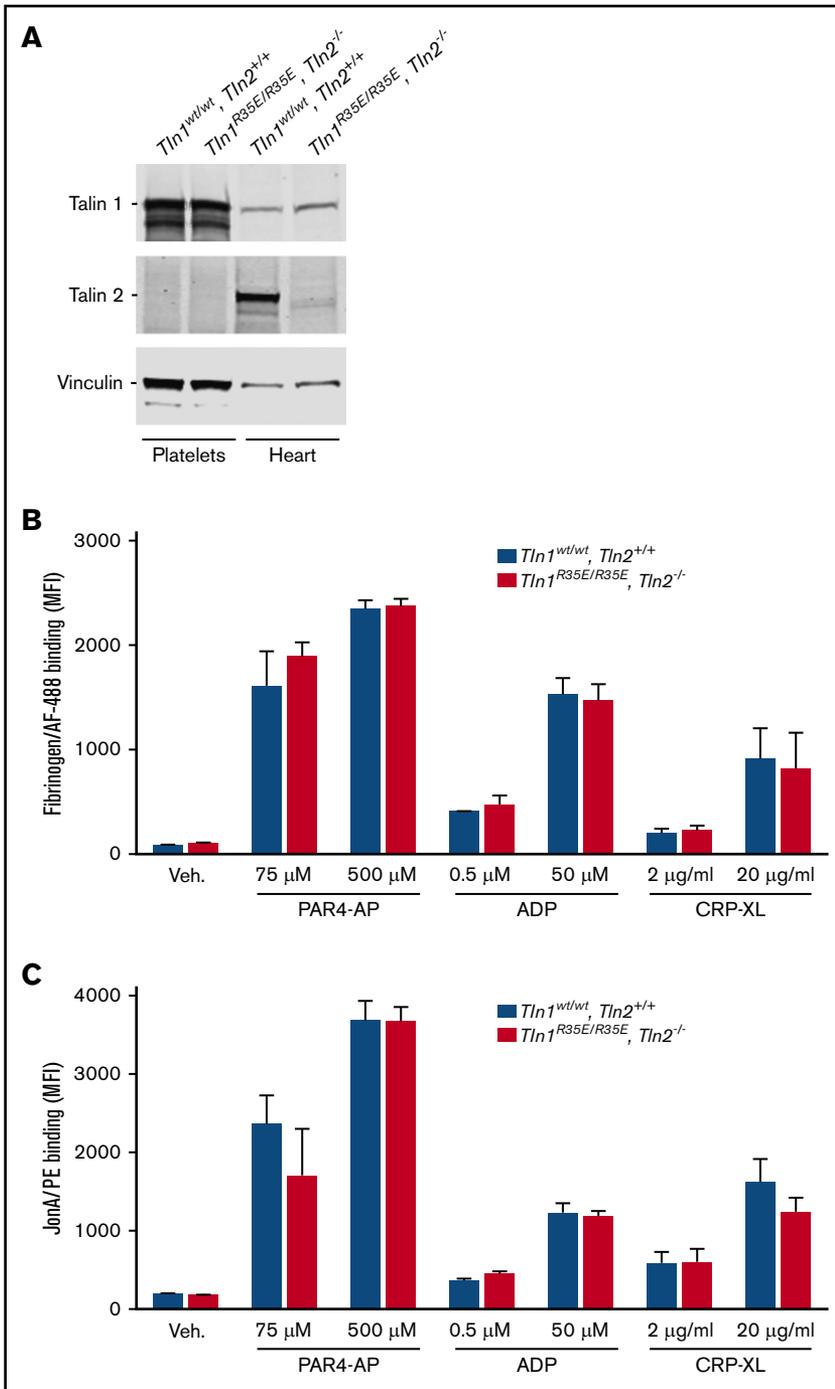
Figure 7. GPIIb-IIIa activation in $Tln1^{R35E/R35E}$, $Tln2^{-/-}$ platelets. (A) Western blot analysis of talin 1 and talin 2 expression in platelets and heart. Vinculin was used as a loading control. Talin 2 is not expressed in platelets. (B-C) Normal GPIIb-IIIa integrin activation in $Tln1^{R35E/R35E}$, $Tln2^{-/-}$ platelets. Flow cytometry assay to measure binding of washed platelets to fibrinogen (B) or GPIX-labeled platelets in whole blood to Jon/A antibody (C). Bar graphs represent MFI ± SEM (n = 3 mice, representative of 2 independent experiments).

of GPIIb-IIIa function in $Tln1^{R35E/R35E}$ platelets, we quantified platelet adhesion and spreading on fibrinogen-coated coverslips in response to stimulation with thrombin. There was no difference in the number of adhered platelets (Figure 5B). $Tln1^{R35E/R35E}$ platelets spread and extend lamellipodia to a similar extent as wild-type platelets (Figure 5C). Importantly, there was a slight, but insignificant, prolongation of tail bleeding times in $Tln1^{R35E/R35E}$ mice (Figure 5D), indicating largely intact hemostasis. Together, these data confirm that the activation and hemostatic functions of GPIIb-IIIa are largely intact in $Tln1^{R35E/R35E}$ platelets.

$Tln1^{R35E/R35E}$ mutation is not compensated by RIAM or talin 2

Platelets express little RIAM.[10,15,23] However, it is possible that upregulation of RIAM bridges Rap1 to talin 1(R35E), thereby compensating for the blockade of the direct Rap1/talin 1 interaction. $Tln1^{R35E/R35E}$ platelets exhibited no increase in RIAM expression. Platelets from $Tln1^{R35E/R35E}$-$Apbb1ip^{-/-}$ mice, lacking RIAM, exhibited normal GPIIb-IIIa activation (Figure 6). These data exclude a compensatory role for RIAM. Furthermore, we examined whether talin 2, which is structurally similar to talin 1, could compensate for

the $Tln1^{R35E/R35E}$ mutation. We could not detect talin 2 expression in platelets, confirming previous reports,[25,26] and its expression was not increased in response to the $Tln1^{R35E/R35E}$ mutation (Figure 7). Furthermore, initial GPIIb-IIIa activation in $Tln1^{R35E/R35E};Tln2^{-/-}$ platelets was indistinguishable from control $Tln1^{wt/wt};Tln2^{+/+}$ platelets (Figure 7).

Discussion

Rap1 GTPases play a critical role in triggering talin-mediated platelet GPIIb-IIIa activation. Our studies have critically examined the role of the binding of Rap1 to the talin 1 F0 domain,[13] which has been proposed[15] to account for the link between Rap1 and talin. Using the structure of the Rap1-F0 complex, we created a single F0 point mutant that did not alter F0 folding and documented that it significantly reduced the affinity of the interaction. Using the well-established CHO system, we showed that this mutation did not affect the capacity of THD to activate recombinant αIIbβ3 across a wide range of expression of THD, nor did it alter the effects of manipulating Rap1 activity. To directly test the role of the Rap1–F0 interaction, we generated $Tln1^{R35E/R35E}$ mice and observed negligible effects on GPIIb-IIIa activation by a wide variety of agonists and on resulting hemostasis; however, we observed a mild defect in platelet aggregation. In sum, our studies show that the talin 1 F0–Rap1 interaction makes a minor contribution to the capacity of Rap1 to trigger GPIIb-IIIa activation and resulting hemostasis.

The interaction of talin 1-F0 with Rap1b plays no evident role in THD-induced recombinant αIIbβ3 activation in CHO cells. These cells, termed A5 cells,[27] have come into wide use and were instrumental in showing the role of THD in activation[28] and how RIAM linked Rap1 to talin to activate integrins.[7] Indeed, when Goult et al[13] first reported the Rap1–F0 interaction, we tested a series of mutants predicted to block the interaction, with no effect on αIIbβ3 activation. In repeating these experiments, with careful quantification of THD expression on a per-cell basis by flow cytometry, we have confirmed our earlier results (Figure 2B). A recent study[15] reported conflicting results; however, differences in experimental methods should be noted. In particular, that study used a THD (K15A,R35A) double mutant. We used the acidic Glu mutations because of the predicted stronger effects of charge repulsions between talin 1 F0 and the acidic patch on the surface of Rap1b that mediates their interaction (Figure 1A). Secondly, we carefully monitored the folding of the R35E mutant (Figure 1B), which was a particular concern in light of the instability of the K15E mutant in our hands. This concern also led to a careful assessment of the expression of mutant and wild-type THD (Figure 2B-C), a feature notably absent from the study by Zhu et al.[15] Thus, in A5 cells, a mutant that drastically reduces the Rap1-F0 affinity has little effect on the capacity of THD to activate recombinant αIIbβ3.

The talin 1(R35E) mutant has little effect on platelet GPIIb-IIIa activation or hemostasis. In the present study, we did not observe any consistent effect of $Tln1(R35E)$ on GPIIb-IIIa activation by several agonists that use distinct receptors in washed platelets, as assessed by the binding of fibrinogen or Jon/A, or in whole blood by Jon/A binding. These results were confirmed by the minor effects on platelet aggregation and bleeding time and are in striking contrast to the profound effects of loss of Rap1 activity[6] or talin 1[26,29] or of mutations of β3 that block talin binding.[30] Importantly, our studies definitively exclude the possibility that upregulation of talin 2 or RIAM expression could account for the lack of effect of this mutation. The mild defect in platelet aggregation at low doses of agonist, in the presence of intact GPIIb-IIIa activation, suggests that the talin 1 F0–Rap1 interaction helps to stabilize the capacity of the platelet aggregates to resist the shear forces in the platelet aggregometer; hence, future studies to explore whether this mild aggregation defect confers an antithrombotic benefit seem warranted.

What is the nature of the Rap1 effector that controls talin 1-dependent integrin activation in platelets? Clearly, F0 binds Rap1 with low affinity and, in *Dictyostelium*, appears to have an important functional role.[13-15] The extraordinary abundance of Rap1 and talin 1 in platelets and the absence of any stoichiometrically reasonable Rap1 effector[23] provided a compelling rationale for considering talin 1 F0 as the logical Rap1 effector[15]; however, our results seem to preclude this idea and leave this critical question open. Zhu et al's comprehensive study reported that Rap1 interaction with talin 1 F1 or kindlin2 F0 could not be detected,[15] appearing to rule out these likely candidates. Vinculin interaction with talin 1 can lead to talin 1–integrin interaction and integrin activation[31]; however, vinculin-null platelets exhibit no reduction in GPIIb-IIIa activation,[32] and vinculin-RIAM double-knockout platelets also exhibit no such defect (Brian G. Petrich and M.H.G., unpublished observations). Thus, future studies could be directed at the possibility that Rap1 can influence the talin 1–integrin interaction by triggering a catalytic event that results in a change of membrane lipid composition or a posttranslational modification of talin 1. The present work would exclude the Rap1–talin 1 F0 interaction as playing a critical role in GPIIb-IIIa activation.

Authorship

Contribution: F.L., A.R.G., and M.H.G. conceived the study, designed experiments, interpreted data, and wrote the manuscript; F.L., A.R.G., D.S.P., A.J.V., and M.N.C. performed and analyzed experiments; F.L. designed the CRISPR/Cas9 approach to generate $Tln1^{R35E/R35E}$ mutant mice; H.S. and M.A.L.-R. provided vital reagents and critical expertise; and B.T.G., S.J.S., and W.B. provided decisive expertise and critical advice and edited the manuscript.

Conflict-of-interest disclosure: The authors declare no competing financial interests.

ORCID profiles: A.R.G., 0000-0002-5373-0176; B.T.G., 0000-0002-3438-2807.

Correspondence: Mark H. Ginsberg, Department of Medicine, University of California, San Diego, 9500 Gilman Dr, La Jolla, CA 92093; e-mail: mhginsberg@ucsd.edu.

References

1. Hynes RO. Integrins: bidirectional, allosteric signaling machines. *Cell*. 2002;110(6):673-687.

2. Shattil SJ, Newman PJ. Integrins: dynamic scaffolds for adhesion and signaling in platelets. *Blood*. 2004;104(6):1606-1615.

3. Shattil SJ, Kim C, Ginsberg MH. The final steps of integrin activation: the end game. *Nat Rev Mol Cell Biol*. 2010;11(4):288-300.

4. Chrzanowska-Wodnicka M, Smyth SS, Schoenwaelder SM, Fischer TH, White GC II. Rap1b is required for normal platelet function and hemostasis in mice. *J Clin Invest*. 2005;115(3):680-687.

5. Crittenden JR, Bergmeier W, Zhang Y, et al. CalDAG-GEFI integrates signaling for platelet aggregation and thrombus formation [published correction appears in *Nat Med*. 2004;10(10):1139.] *Nat Med*. 2004;10(9):982-986.

6. Stefanini L, Lee RH, Paul DS, et al. Functional redundancy between RAP1 isoforms in murine platelet production and function primates [published online ahead of print 21 August 2018]. *Blood*. doi:blood-2018-03-838714.

7. Han J, Lim CJ, Watanabe N, et al. Reconstructing and deconstructing agonist-induced activation of integrin alphaIIbbeta3. *Curr Biol*. 2006;16(18):1796-1806.

8. Lafuente EM, van Puijenbroek AA, Krause M, et al. RIAM, an Ena/VASP and profilin ligand, interacts with Rap1-GTP and mediates Rap1-induced adhesion. *Dev Cell*. 2004;7(4):585-595.

9. Lee HS, Lim CJ, Puzon-McLaughlin W, Shattil SJ, Ginsberg MH. RIAM activates integrins by linking talin to ras GTPase membrane-targeting sequences. *J Biol Chem*. 2009;284(8):5119-5127.

10. Klapproth S, Sperandio M, Pinheiro EM, et al. Loss of the Rap-1 effector RIAM results in leukocyte adhesion deficiency due to impaired beta2 integrin function in mice. *Blood*. 2015;126(25):2704-2712.

11. Stritt S, Wolf K, Lorenz V, et al. Rap1-GTP-interacting adaptor molecule (RIAM) is dispensable for platelet integrin activation and function in mice. *Blood*. 2015;125(2):219-222.

12. Su W, Wynne J, Pinheiro EM, et al. Rap1 and its effector RIAM are required for lymphocyte trafficking. *Blood*. 2015;126(25):2695-2703.

13. Goult BT, Bouaouina M, Elliott PR, et al. Structure of a double ubiquitin-like domain in the talin head: a role in integrin activation. *EMBO J*. 2010;29(6):1069-1080.

14. Plak K, Pots H, Van Haastert PJ, Kortholt A. Direct interaction between talinB and Rap1 is necessary for adhesion of *Dictyostelium* cells. *BMC Cell Biol*. 2016;17:1.

15. Zhu L, Yang J, Bromberger T, et al. Structure of Rap1b bound to talin reveals a pathway for triggering integrin activation. *Nat Commun*. 2017;8(1):1744.

16. Gingras AR, Puzon-McLaughlin W, Bobkov AA, Ginsberg MH. Structural basis of dimeric Rasip1 RA domain recognition of the Ras subfamily of GTP-binding proteins. *Structure*. 2016;24(12):2152-2162.

17. Vranken WF, Boucher W, Stevens TJ, et al. The CCPN data model for NMR spectroscopy: development of a software pipeline. *Proteins*. 2005;59(4):687-696.

18. Frojmovic MM, O'Toole TE, Plow EF, Loftus JC, Ginsberg MH. Platelet glycoprotein IIb-IIIa (alpha IIb beta 3 integrin) confers fibrinogen- and activation-dependent aggregation on heterologous cells. *Blood*. 1991;78(2):369-376.

19. Shattil SJ, Hoxie JA, Cunningham M, Brass LF. Changes in the platelet membrane glycoprotein IIb.IIIa complex during platelet activation. *J Biol Chem*. 1985;260(20):11107-11114.

20. O'Toole TE, Katagiri Y, Faull RJ, et al. Integrin cytoplasmic domains mediate inside-out signal transduction. *J Cell Biol*. 1994;124(6):1047-1059.

21. Conti FJ, Monkley SJ, Wood MR, Critchley DR, Müller U. Talin 1 and 2 are required for myoblast fusion, sarcomere assembly and the maintenance of myotendinous junctions. *Development*. 2009;136(21):3597-3606.

22. Scrima A, Thomas C, Deaconescu D, Wittinghofer A. The Rap-RapGAP complex: GTP hydrolysis without catalytic glutamine and arginine residues. *EMBO J*. 2008;27(7):1145-1153.

23. Zeiler M, Moser M, Mann M. Copy number analysis of the murine platelet proteome spanning the complete abundance range. *Mol Cell Proteomics*. 2014; 13(12):3435-3445.

24. Bergmeier W, Schulte V, Brockhoff G, Bier U, Zirngibl H, Nieswandt B. Flow cytometric detection of activated mouse integrin alphaIIbbeta3 with a novel monoclonal antibody. *Cytometry*. 2002;48(2):80-86.

25. Monkley SJ, Pritchard CA, Critchley DR. Analysis of the mammalian talin 2 gene TLN2. *Biochem Biophys Res Commun*. 2001;286(5):880-885.

26. Petrich BG, Marchese P, Ruggeri ZM, et al. Talin is required for integrin-mediated platelet function in hemostasis and thrombosis. *J Exp Med*. 2007; 204(13):3103-3111.

27. O'Toole TE, Loftus JC, Du XP, et al. Affinity modulation of the alpha IIb beta 3 integrin (platelet GPIIb-IIIa) is an intrinsic property of the receptor. *Cell Regul*. 1990;1(12):883-893.

28. Calderwood DA, Zent R, Grant R, Rees DJ, Hynes RO, Ginsberg MH. The talin head domain binds to integrin beta subunit cytoplasmic tails and regulates integrin activation. *J Biol Chem*. 1999;274(40):28071-28074.

29. Nieswandt B, Moser M, Pleines I, et al. Loss of talin 1 in platelets abrogates integrin activation, platelet aggregation, and thrombus formation in vitro and in vivo. *J Exp Med*. 2007;204(13):3113-3118.

30. Petrich BG, Fogelstrand P, Partridge AW, et al. The antithrombotic potential of selective blockade of talin-dependent integrin alpha IIb beta 3 (platelet GPIIb-IIIa) activation. *J Clin Invest*. 2007;117(8):2250-2259.

31. Lee HS, Anekal P, Lim CJ, Liu CC, Ginsberg MH. Two modes of integrin activation form a binary molecular switch in adhesion maturation. *Mol Biol Cell*. 2013;24(9):1354-1362.

32. Mitsios JV, Prevost N, Kasirer-Friede A, et al. What is vinculin needed for in platelets? *J Thromb Haemost*. 2010;8(10):2294-2304.